

Deep mesoscale eddies in the Canada Basin, Arctic Ocean

J. R. Carpenter¹ and M.-L. Timmermans¹

Received 12 July 2012; revised 12 September 2012; accepted 13 September 2012; published 17 October 2012.

[1] Numerous eddies have been identified in a seven year time series of mooring observations in the Canada Basin, Arctic Ocean. We focus on a series of deep eddies centered at ~ 1200 m depth, and occupying up to 1500 m of the water column. The deep eddies are found to be spatially localized, only ever being observed at one of four mooring sites of the Beaufort Gyre Observing System in the Canada Basin. However, despite only a few previously reported observations of deep eddies in the Arctic Ocean, we find that they are the most prevalent eddy-type at this location. Based on this observation, together with an analysis of the temperature-salinity structure, and the exclusively anticyclonic rotation of the deep eddies, we hypothesize that they are formed by a density-driven outflow from the Chukchi Borderland region. We also describe a simple analytical model to explain the observed vertical scales of the eddies. **Citation:** Carpenter, J. R., and M.-L. Timmermans (2012), Deep mesoscale eddies in the Canada Basin, Arctic Ocean, *Geophys. Res. Lett.*, 39, L20602, doi:10.1029/2012GL053025.

1. Introduction

[2] The Arctic Ocean is known for exhibiting strong mesoscale eddy activity [Newton *et al.*, 1974; Manley and Hunkins, 1985; D'Asaro, 1988a; Muench *et al.*, 2000; Pickart *et al.*, 2005; Timmermans *et al.*, 2008; Spall *et al.*, 2008]. In fact, Manley and Hunkins [1985] estimate that mesoscale eddies can occupy up to one quarter of the surface area of the Beaufort Sea. However, the vast majority of the eddies have been observed to be confined to depths within the relatively shallow halocline from near the surface to ~ 200 m. Various formation mechanisms have been proposed for these shallow eddies such as instabilities associated with dense water formation at polynyas [Muench *et al.*, 2000], instabilities of frontal regions [Timmermans *et al.*, 2008], instabilities of the shelfbreak jet [Pickart *et al.*, 2005; Spall *et al.*, 2008], and current interaction with topography [D'Asaro, 1988b]. Despite the prominence of shallow halocline eddies in the literature, some exceptions to this have been noted in a series of isolated observations of eddy features with center depths ranging from ~ 600 m to ~ 1800 m [Swift *et al.*, 1997; Woodgate *et al.*, 2001; Schauer *et al.*, 2002; Aagaard *et al.*, 2008]. For example, Aagaard *et al.* [2008] have recently described observations of an anticyclonic mesoscale eddy in the Eurasian Basin that extends throughout

a depth of ~ 1500 m, with a maximum velocity at, or below, a depth of ~ 600 m.

[3] In this paper, we present time series data spanning approximately 7 years from moorings located in the Canada Basin of the Arctic Ocean. The observations indicate that mesoscale eddies can be a common feature of the water column between 500 and 2000 m. However, these eddies are found to be spatially concentrated in an area close to the northern region of the Northwind Ridge (see Figure 1a). Based on these observations, as well as the unique temperature-salinity structure of the eddy cores, we propose a mechanism for their formation based on a buoyancy-driven outflow from the Northwind Abyssal Plain (NWAP). This mechanism for deep eddy formation, first described by Spall and Price [1998] for Denmark Strait, appears to be in general agreement with the isolated observations of Swift *et al.* [1997], Woodgate *et al.* [2001], and Schauer *et al.* [2002], who observe deep eddies with water mass properties that have their origin in different basins of the Arctic Ocean. Our proposed mechanism for deep eddy formation would support the theory that much of the inter-basin exchange within the Arctic Ocean, due to inflows and outflows over and through topography, takes place through mesoscale eddy transport. In addition, we present a simple model to understand and predict the origin of the large vertical scales of the observed deep eddies.

2. Measurements

[4] The primary measurements that we will discuss are from four moorings located in the Canada Basin as part of the Beaufort Gyre Observing System (BGOS, <http://www.whoi.edu/beaufortgyre>, and see Proshutinsky *et al.* [2009]). BGOS moorings are denoted by the letters shown in Figure 1a, with most of the measurements we discuss from mooring B. On each mooring a McLane Moored Profiler (MMP) measures conductivity, temperature, depth and the two components of horizontal velocity, with profiles alternately separated by 6 and 48 hours, spanning an approximate depth range of 50–2000 m. Accuracy of the MMP salinity data is better than 0.005 g kg^{-1} [Proshutinsky *et al.*, 2009]. In addition to the mooring data, we also use CTD data collected from the Chukchi Borderland (CBL) expedition in 2002 [Woodgate *et al.*, 2007] and CTD stations carried out during the Beringia/HOTRAX 2005 expedition from icebreaker Oden [see Jones *et al.*, 2008].

3. Deep Eddies

[5] Measurements taken from mooring B, located close to the Northwind Ridge and Chukchi Borderland region, are shown over the 7 year time series in Figure 2. The presence of many different eddies can be seen in both the magnitude of the horizontal velocity $|\mathbf{u}| = (u^2 + v^2)^{1/2}$ (Figure 2a), and in the conservative temperature, Θ ($^{\circ}\text{C}$), and density fields

¹Department of Geology and Geophysics, Yale University, New Haven, Connecticut, USA.

Corresponding author: J. R. Carpenter, Department of Geology and Geophysics, Yale University, 210 Whitney Ave., New Haven, CT 06511, USA. (jeffcarp@gmail.com)

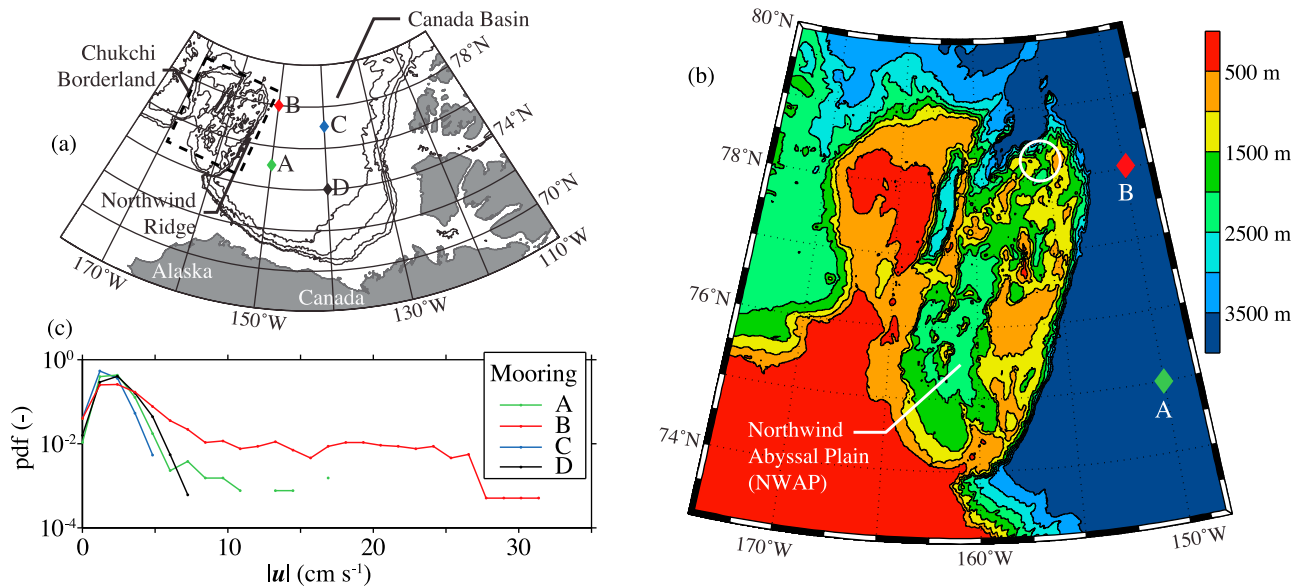


Figure 1. (a) Map with the locations of the four moorings and the bathymetry of the Canada Basin. (b) The bathymetry of the Chukchi Borderland and Northwind Abyssal Plain (NWAP) regions [Jakobsson *et al.*, 2012]. The white circle indicates a gap in the NWAP basin. (c) Probability density functions of $|u|$ at 1200 m, the approximate center depth of the deep eddies, for each of the four moorings in the Canada Basin.

(Figure 2b). The eddies can generally be classified into three different depth regions: (i) shallow upper halocline eddies centered at ~ 80 m depth, (ii) lower halocline eddies (~ 200 m depth), and (iii) deep eddies (~ 1200 m depth). The deep eddies occur most frequently at mooring B, and all share a number of similar characteristics: they are all centered at a similar depth (~ 1200 m), have a similar velocity structure extending between 1–2 km in the vertical, are anticyclonic with isopycnals displaced upwards above the eddy center and downwards below, and consist of anomalously cold water above the center and anomalously warm below. These similarities suggest that they are all derived from the same source.

Note that in contrast, the lower halocline eddies (~ 200 m depth) display both warm and cold anomalies.

[6] We estimate the radii of the deep eddies by a kinematic method similar to Lilly and Rhines [2002]. The eddies are assumed to be composed of a core region that is in solid body rotation with radius R . The core is therefore composed of fluid with a constant relative vorticity given by V/R , where V is the maximum azimuthal velocity at the edge of the core. Since the mooring is at a fixed location, and the eddies are intersecting it as they move within the basin, if an eddy core is to pass through the mooring it should record two local maxima in $|u|$. If the core does not pass through the mooring

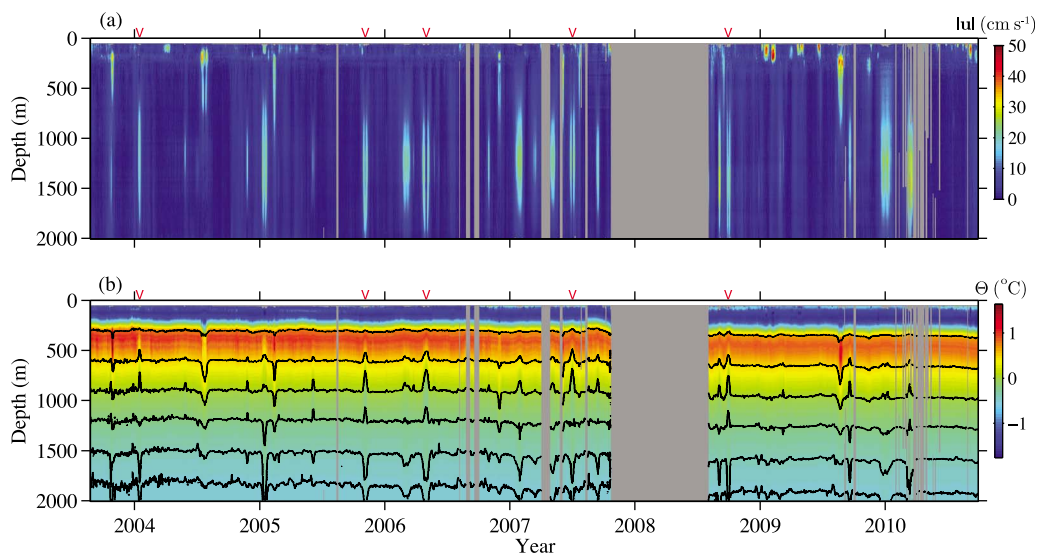


Figure 2. Time series of (a) horizontal velocity magnitude $|u|$ (cm s^{-1}), and (b) conservative temperature Θ ($^{\circ}\text{C}$), taken at mooring B. The dark gray regions indicate times and depths with no profiler information. The dark contours in Figure 2b are isopycnals chosen to be spaced evenly in depth at the start of the record. The red markers indicate the times of the 5 eddy cores in Table 1.

Table 1. Summary of Estimated Eddy Scales and Rossby Numbers for Five Deep Eddies Whose Cores have Intersected Mooring B

Date	V (cm s^{-1})	R (km)	Ro (-)
14 January, 2005	23–24	17–25	0.13–0.20
3 November, 2005	22	12–13	0.23–0.25
30 April, 2006	24	18–20	0.17–0.19
2 July, 2007	26	11–21	0.18–0.32
28 September, 2008	19	12–13	0.20–0.23

then only a single maximum in $|\mathbf{u}|$ is recorded. Of the approximately 20 deep eddy events recorded at mooring B, only five cores were found to significantly intersect the mooring. The mean background current speed ($\sim 1\text{--}2 \text{ cm s}^{-1}$) is assumed responsible for passively advecting the eddy, and is estimated by averaging the measured currents at the mooring over the depth range of 1100–1300 m. This is done for three days (6 profiles) immediately before and after the passage of the eddy, and gives a range of possible advection speeds. Note that at these latitudes the self-propagation of the eddies is expected to be small ($< 0.1 \text{ cm s}^{-1}$), which is given approximately by the first-mode baroclinic Rossby wave speed [Chelton *et al.*, 2011]. For each of the five eddy events we determine R based on the best fit of the measured $|\mathbf{u}|$ at the mooring, and that predicted with a core in solid-body rotation. The range of possible advection speeds, and choices for V , lead to a range in the prediction of R . Table 1 summarizes the results of the eddy core size calculations.

[7] Based on the relative vorticity magnitude V/R and the Coriolis frequency f , we can form a characteristic eddy Rossby number, $Ro \equiv 2V/Rf$. In agreement with previous studies of deep eddies [Lilly and Rhines, 2002; Aagaard *et al.*, 2008], we find $Ro \approx 0.2$, indicating that the eddy is close to geostrophic balance. The eddy radii, $11 \leq R \leq 25 \text{ km}$, are therefore also of the same order as the first baroclinic Rossby radius, $L_R = NH/f \approx 11 \text{ km}$. Here the eddy vertical height $H \approx 1.5 \text{ km}$, and the buoyancy frequency $N(z)$, defined through $N^2(z) = (g/\rho_0) \partial\rho/\partial z$, is taken as $N \approx 10^{-3} \text{ s}^{-1}$, representative of 1200 m depth. Our estimated values of R are also in agreement with the $8 < R < 16 \text{ km}$ range found for the deep eddy described in Aagaard *et al.* [2008].

[8] Observations from the other three moorings in the Canada Basin (A,C,D in Figure 1a) show that the deep eddies are not present in these other areas. This can be seen in the probability density function (pdf) of horizontal velocity magnitude ($|\mathbf{u}|$) taken at the depth of 1200 m, shown in Figure 1c. In each mooring the relatively quiet background circulation below the halocline can be characterized by horizontal velocities predominantly between 0 and 5 cm s^{-1} . However, only at mooring B are large velocities in excess of 10 cm s^{-1} frequently observed. These large velocities are due to deep eddies frequently passing through mooring B, and indicate that the eddies are spatially localized in this region. Chelton *et al.* [2011] have estimated that midlatitude eddies with $R < 67 \text{ km}$ typically have lifetimes of 8 weeks or less. At an advection speed between 1 and 2 cm s^{-1} , this results in a travel distance of 50 to 100 km from the point of origin. Therefore, the eddies are not expected to be observed in the other moorings located $> 250 \text{ km}$ away. Only eddies lasting longer than 6 months would be expected to be observed in the other moorings. It is possible however, that

the high $|\mathbf{u}|$ tail in the pdf observed at mooring A, may be due to a single deep eddy.

[9] An examination of the temperature-salinity characteristics (using Θ and absolute salinity, S_A , in g kg^{-1}) of the five deep eddy cores that have intersected mooring B, shows that they have a similar and unique structure (Figure 3b, red curves). These eddy core profiles are compared with other profiles from the Chukchi Borderland region, and over the Canada Basin abyssal plain, in Figure 3. We identify three principle water masses of interest that are present at depths below $\sim 600 \text{ m}$: (i) Canada Basin boundary current water that resides on the shelf break and has its origin in the North Atlantic and Barents Sea (Figure 3, in purple) [Woodgate *et al.*, 2007; McLaughlin *et al.*, 2009], (ii) Canada Basin interior water (in black), and (iii) topographically isolated “relic” water in the deep region of the NWP (in green) [Woodgate *et al.*, 2007]. The eddy core profiles cannot be characterized by any single water mass; they instead appear to consist of NWP water below their cores (denser than $\sigma_{1000} = 32.76 \text{ kg m}^{-3}$), with boundary current and basin interior waters above. An exception is the eddy of 28 September, 2008, which does not clearly show the presence of boundary current waters near the core. This may be due to the eddy core not passing close enough to mooring B. As shown in Figure 3d, the NWP waters below the cores are not observed at mooring B at any time unless associated with the core of a deep eddy.

4. Interpretation

[10] We propose that the deep eddies observed at mooring B are the result of an outflow from the NWP region into the Canada Basin boundary current and interior. This mechanism for the formation of the deep eddies explains the temperature-salinity structure of the eddies, the exclusively anticyclonic rotation, as well as their concentration at mooring B. Various components of this interpretation are illustrated diagrammatically in Figure 4, which we shall now discuss.

[11] Profiles of potential density anomaly measured from inside the NWP are seen to consist of relatively lighter water than any profiles measured in the boundary current or basin interior (Figure 3c). This is generally true below a depth of $\sim 1500 \text{ m}$, and in the case of one profile, below a depth of $\sim 1300 \text{ m}$. Due to the presence of gaps in the topography (one such gap can be seen on Figure 1b with a maximum depth of $\sim 1700 \text{ m}$) close to the level that NWP water shows density differences, the lighter NWP water can outflow at its level of neutral buoyancy. Since the stratification within the NWP is less than that in the Canada Basin (Figure 3c), a significant compression of the outflowing water column will result, causing a local increase in the relative vorticity, ζ . This increase in ζ is needed in order for the outflow to conserve potential vorticity (PV) defined by $q \equiv (\zeta + f)/h$ in the case of a layered density stratification, where h is the depth of the layer in question. For the outflow to conserve q under a compression it must acquire an anticyclonic ($\zeta < 0$) rotation. Assuming that the outflowing water, with initial depth h_1 , begins with no relative vorticity, we can determine the amount of compression needed to produce the vorticity anomaly of the observed eddies. Using the conservation of PV gives a relative compression of $(h_1 - h_2)/h_1 = Ro/2$, where h_2 is the final depth of the compressed outflow. With the observation of $Ro \approx 0.2$ we find

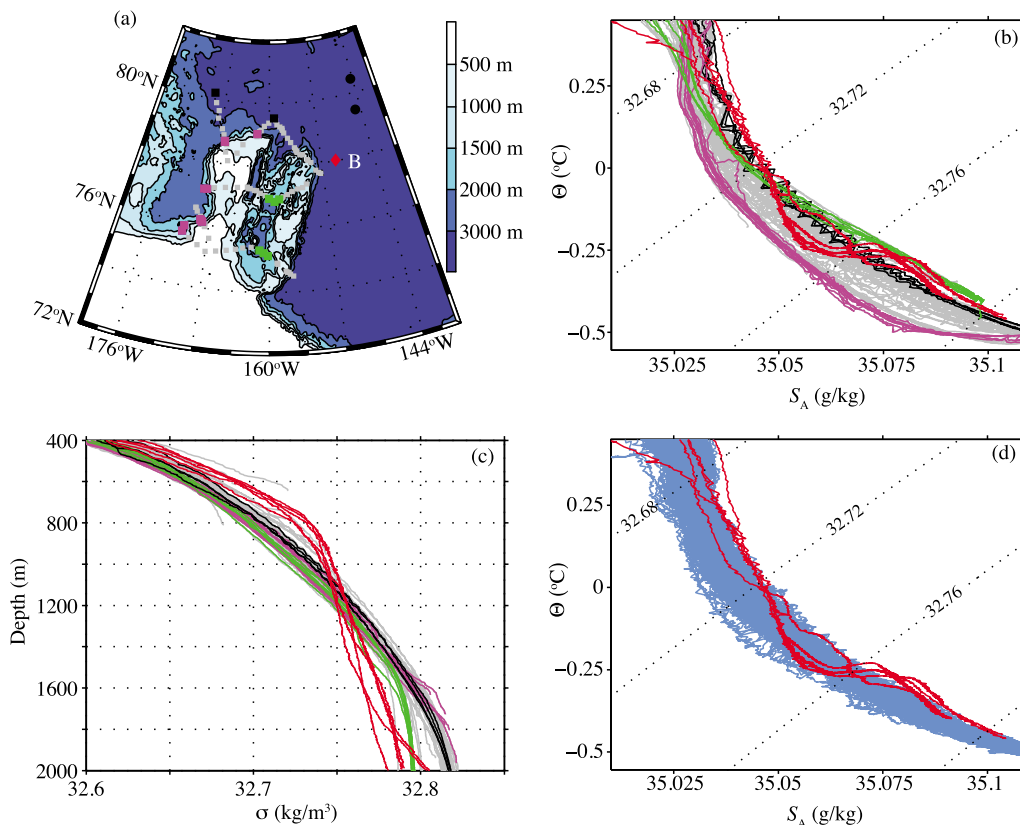


Figure 3. (a) Map of the Chukchi Borderland region and the location of CTD casts from the CBL2002 data set (square symbols) and the Beringia/HOTRAX 2005 data set (black circular symbols). The color contours represent depth and the location of mooring B is shown in red. (b) Conservative temperature (Θ) vs. absolute salinity (S_A) plot showing the profiles corresponding to the colored and gray symbols in Figure 3a. The five red curves are measurements at mooring B from the cores of eddies from different years (see Table 1). (c) Profiles of potential density anomaly $\sigma_{1000} = \rho - 1000$ with the potential density, ρ , referenced to 1000 m depth, and gray and colored lines corresponding to the symbols in Figure 3a. (d) $\Theta - S_A$ plot showing the eddy core profiles (in red) against the quiet background at mooring B (blue) for the duration of the measurements.

$(h_1 - h_2)/h_1 \approx 0.1$. Therefore, even a relative compression of only 10% of the outflowing water column would be enough to produce the observed vorticity anomaly of the deep eddies. Based on the thickness of the layer of NWAP water inside the deep eddy cores (inferred from the $\Theta - S_A$ plot in Figure 3b), we estimate $h_2 \approx 200$ m, and an initial column depth for the outflow of $h_1 \approx 220$ m is required. It can be seen from Figure 3c that this 220 m column of less dense NWAP water is available for the exchange.

[12] The existence of an exchange between the NWAP and the boundary current of the Canada Basin was first suggested by *Woodgate et al.* [2007]. Based on a water mass analysis they proposed that the exchange occurs through numerous gaps in the topography towards the northern region of the NWAP. Despite the existence of this exchange process, the waters of the NWAP are generally believed to be topographically trapped by the surrounding ridges, most of which reach depths of ~ 1000 m or less, and this has led *Woodgate et al.* [2007] to refer to them as “relic” waters. The exchange that we are proposing with these waters and the boundary current does not contradict this description. Based on the observed frequency of the deep eddies (20 eddies over 6.3 years), and the approximate volume of NWAP waters in them (250 km^3 , from $R = 20 \text{ km}$ and a depth of $\Delta h \approx 200 \text{ m}$) we estimate a transport rate of $800 \text{ km}^3 \text{ yr}^{-1}$. Together with a

NWAP volume estimate of $9.5 \times 10^4 \text{ km}^3$ below 1200 m, this gives a renewal time of 120 years. Note that this estimate assumes that all of the eddies generated by the outflow have passed by the mooring, and likely represents an overestimate.

[13] If there is an exchange flow between the Canada Basin and the NWAP, then it is useful to estimate possible rates of inflow to the NWAP. We assume a hydraulically controlled deep inflow occurs through the gap identified in Figure 1b with a maximum depth at 1700 m, an inflowing layer of thickness $h_i = 200$ m (since the density profiles are similar above 1500 m), and a density difference given by the

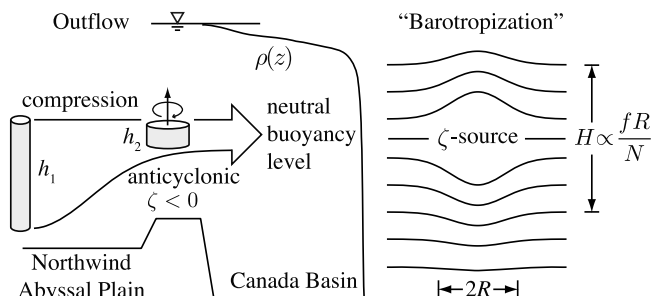


Figure 4. Illustration of the proposed deep eddy formation process.

difference between the NWP and basin interior means at the approximate 1700 m depth of the sill, $\Delta\rho = 0.012 \text{ kg m}^{-3}$ (Figure 3c). The resulting flow rate is given by *Whitehead* [1998] as $\mathcal{V} = g' h_i^2 / 2f$, where $g' = \Delta\rho g / \rho_0$ is the reduced gravity, with g the gravitational acceleration, and $\rho_0 = 1033 \text{ kg m}^{-3}$ a reference density. This formula assumes that the width of the exchange channel is greater than the internal Rossby radius for the NWP inflow $(2g'h_i)^{1/2}/f = 1.5 \text{ km}$, and gives an estimated flow of $520 \text{ km}^3 \text{ yr}^{-1}$, or a residence time of 180 years, in reasonable agreement with our previous estimate. However, there remains the open question of what processes are responsible for replenishing the relatively lighter deep waters of the NWP from the hypothesized dense inflows of the Canada Basin.

[14] Although the anticyclonic vorticity source for the deep eddies may be concentrated in a narrow depth range at the level of the outflow, a “barotropization” process will take place in which the eddies adjust their vertical structure to the weakly stratified environment of the deep Canada Basin. A representative vertical scale height for the eddies can be found by applying the conservation of PV once again. For a rotating and continuously stratified flow on an f -plane the quasi-geostrophic PV is expressed as

$$q = \frac{\partial^2 \psi}{\partial x^2} + \frac{\partial^2 \psi}{\partial y^2} + \frac{\partial}{\partial z} \left(\frac{f^2}{N^2(z)} \frac{\partial \psi}{\partial z} \right), \quad (1)$$

where ψ is the streamfunction defined by $u = \partial\psi/\partial y$ and $v = -\partial\psi/\partial x$. For purposes of illustration, we take $N(z)$ to be constant and seek steady solutions to the linearized form of the conservation of PV. This is a form of the classical geostrophic adjustment problem, and once a scaled vertical coordinate $z_* = z(N/f)$ is defined, reduces to a Poisson equation

$$\nabla^2 \psi = Q(x, y, z_*), \quad (2)$$

given some distribution of vorticity $Q(x, y, z_*)$. Solutions to (2) are found by taking $\psi(x, y, z_*) = \hat{\psi}(z_*) \exp(ikx + ily)$, where k and l are wavenumbers in the horizontal x and y directions. If we take Q to be concentrated at the outflow level z_0 (given by a delta function) and assume an ocean of infinite depth, then the eddy velocity and density perturbation fields have an exponential decay from this level given by $\exp[-(KN/f)|z - z_0|]$, with $K = (k^2 + l^2)^{1/2}$ the magnitude of the horizontal wavenumber. This shows that if the vertical scale, H , of the eddies is defined to be the height over which the eddy decays to within 90% of the background then

$$H = \frac{\ln(10)Rf}{\pi N}, \quad (3)$$

where we have used $R = 2\pi/K$ as the horizontal eddy scale. Substituting some approximate values of $N \approx 10^{-3} \text{ s}^{-1}$ (representative of 1200 m), $f = 1.4 \times 10^{-4} \text{ s}^{-1}$, and $R \approx 20 \text{ km}$, gives a rough estimate of $H \approx 2000 \text{ m}$, in good agreement with the observations. The relation in (3) may be stated alternatively as a condition on the Burger number, $Bu \equiv (NH/fR)^2 = (L_R/R)^2 \approx \text{constant}$, as observed previously by *D'Asaro* [1988a].

[15] This simple analysis shows that the large vertical scales of the deep eddies are due to the low N/f ratios that are present in the deep Arctic Ocean, with H scaling as fR/N . The

“barotropization” process that the eddies must undergo in the weakly stratified water column below the halocline can also be seen in the shallower lower-halocline eddies of Figure 2. When the eddies are deep enough to penetrate below the base of the strongly stratified halocline at $\sim 200 \text{ m}$, the low N/f environment causes the vertical structure of mesoscale features to extend to great depths.

[16] In summary, we have found that the water column of the Canada Basin, below the strongly stratified halocline, is populated by numerous deep mesoscale eddies. The central core of the eddies contains water that is likely from the NWP region of the Chukchi Borderland, and leads us to propose that the deep eddies are formed from a buoyancy-driven outflow. Even a relatively small amount of water column compression associated with this outflow will generate the observed anticyclonic vorticity anomaly of the eddies. A “barotropization” process will then set the vertical scale of the eddies to $H \propto fR/N$, maintaining a constant Burger number. Future work should focus on elucidating the general process of eddy formation (cyclogenesis) within outflows of the Arctic Ocean to assess its relevance to inter-basin transport mechanisms.

[17] **Acknowledgments.** Moored data were provided by the U.S. National Science Foundation Beaufort Gyre Observing System (BGOS, <http://www.whoi.edu/beaufortgyre/>). We thank Andrey Proshutinsky, Rick Krishfield, and John Toole for essential support and valuable discussions. We also thank Natalie Burls, Geogy Manucharyan, Les Muir, Claudia Cenedese, and Geoffrey Vallis for helpful discussions. Funding for the analysis was provided by Yale University and by the National Science Foundation Office of Polar Programs under award ARC-0806306. We appreciate the support of the captain and crew of the Canadian Coast Guard icebreaker, Louis S. St-Laurent, and we acknowledge financial and ship time support from Fisheries and Oceans Canada, the Canadian International Polar Year Program's Canada's Three Oceans project, and by the NSF BGOS and collaboration with the Japan Agency for Marine-Earth Science and Technology. Data from the Chukchi Borderland Cruise CBL2002 and from the Oden Beringia 2005 expedition were also used in this analysis.

[18] The Editor thanks two anonymous reviewers for assistance evaluating this manuscript.

References

- Aagaard, K., R. Anderson, J. Swift, and J. Johnson (2008), A large eddy in the central Arctic Ocean, *Geophys. Res. Lett.*, *35*, L09601, doi:10.1029/2008GL033461.
- Chelton, D. B., M. G. Schlax, and R. M. Samelson (2011), Global observations of nonlinear mesoscale eddies, *Prog. Oceanogr.*, *91*, 167–216.
- D'Asaro, E. (1988a), Observations of small eddies in the Beaufort Sea, *J. Geophys. Res.*, *93*, 6669–6684.
- D'Asaro, E. (1988b), Generation of submesoscale vortices: A new mechanism, *J. Geophys. Res.*, *93*(C6), 6685–6693.
- Jakobsson, M., et al. (2012), The international bathymetric chart of the Arctic Ocean (IBCAO) version 3.0, *Geophys. Res. Lett.*, *39*, L12609, doi:10.1029/2012GL052219.
- Jones, E., L. Anderson, S. Jutterström, L. Mintrop, and J. Swift (2008), Pacific freshwater, river water and sea ice meltwater across Arctic Ocean basins: Results from the 2005 Beringia Expedition, *J. Geophys. Res.*, *113*, C08012, doi:10.1029/2007JC004124.
- Lilly, J. M., and P. B. Rhines (2002), Coherent eddies in the Labrador Sea observed from a mooring, *J. Phys. Oceanogr.*, *32*, 585–598.
- Manley, T., and K. Hunkins (1985), Mesoscale eddies of the Arctic Ocean, *J. Geophys. Res.*, *90*, 4911–4930.
- McLaughlin, F., E. Carmack, W. Williams, S. Zimmermann, K. Shimada, and M. Itoh (2009), Joint effects of boundary currents and thermohaline intrusions on the warming of the Atlantic water in the Canada Basin, 1993–2007, *J. Geophys. Res.*, *114*, C00A12, doi:10.1029/2008JC005001.
- Muench, R., J. Gunn, T. Whitedge, P. Schlosser, and W. Smethie Jr. (2000), An Arctic Ocean cold core eddy, *J. Geophys. Res.*, *105*(C10), 23,997–24,006.
- Newton, J., K. Aagaard, and L. Coachman (1974), Baroclinic eddies in the Arctic Ocean, *Deep Sea Res.*, *21*, 707–719.

- Pickart, R., T. Weingartner, L. Pratt, S. Zimmermann, and D. Torres (2005), Flow of winter-transformed Pacific water into the Western Arctic, *Deep Sea Res., Part II*, 52, 3175–3198.
- Proshutinsky, A., et al. (2009), Beaufort Gyre freshwater reservoir: State and variability from observations, *J. Geophys. Res.*, 114, C00A10, doi:10.1029/2008JC005104.
- Schauer, U., B. Rudels, E. Jones, L. Anderson, R. Muench, G. Björk, J. Swift, V. Ivanov, and A.-M. Larsson (2002), Confluence and redistribution of Atlantic water in the Nansen, Admundsen and Marakov basins, *Ann. Geophys.*, 20, 257–273.
- Spall, M., and J. Price (1998), Mesoscale variability in Denmark Strait: The PV outflow hypothesis, *J. Phys. Oceanogr.*, 28, 1598–1623.
- Spall, M., R. Pickart, P. Fratantoni, and A. Plueddemann (2008), Western Arctic shelfbreak eddies: Formation and transport, *J. Phys. Oceanogr.*, 38, 1644–1668.
- Swift, J., E. Jones, K. Aagaard, E. Carmack, H. Hingston, R. MacDonald, F. McLaughlin, and R. Perkin (1997), Waters of the Marakov and Canada basins, *Deep Sea Res., Part II*, 44(8), 1503–1529.
- Timmermans, M.-L., J. Toole, A. Proshutinsky, R. Krishfield, and A. Plueddemann (2008), Eddies in the Canada Basin, Arctic Ocean, observed from ice-tethered profilers, *J. Phys. Oceanogr.*, 38, 133–145.
- Whitehead, J. A. (1998), Topographic control of oceanic flows in deep passages and straits, *Rev. Geophys.*, 36, 423–440.
- Woodgate, R., K. Aagaard, R. Muench, J. Gunn, G. Björk, B. Rudels, A. Roach, and U. Schauer (2001), The Arctic Ocean boundary current along the Eurasian slope and the adjacent Lomonosov Ridge: Water mass properties, transports and transformations from moored instruments, *Deep Sea Res., Part I*, 48, 1757–1792.
- Woodgate, R., K. Aagaard, J. Swift, W. M. Smethie Jr., and K. Falkner (2007), Atlantic water circulation over the Mendeleev Ridge and Chukchi Borderland from thermohaline intrusions and water mass properties, *J. Geophys. Res.*, 112, C02005, doi:10.1029/2005JC003416.